Stabilization of time domain acoustic boundary element method for the exterior problem avoiding the nonuniqueness

Hae-Won Jang and Jeong-Guon Ih[a)]
Center for Noise and Vibration Control, Department of Mechanical Engineering, Korea Advanced Institute of Science and Technology, Daejeon 305-701, Korea

(Received 30 July 2012; revised 12 November 2012; accepted 21 December 2012)

The time domain boundary element method (TBEM) to calculate the exterior sound field using the Kirchhoff integral has difficulties in non-uniqueness and exponential divergence. In this work, a method to stabilize TBEM calculation for the exterior problem is suggested. The time domain CHIEF (Combined Helmholtz Integral Equation Formulation) method is newly formulated to suppress low order fictitious internal modes. This method constrains the surface Kirchhoff integral by forcing the pressures at the additional interior points to be zero when the shortest retarded time between boundary nodes and an interior point elapses. However, even after using the CHIEF method, the TBEM calculation suffers the exponential divergence due to the remaining unstable high order fictitious modes at frequencies higher than the frequency limit of the boundary element model. For complete stabilization, such troublesome modes are selectively adjusted by projecting the time response onto the eigenspace. In a test example for a transiently pulsating sphere, the final average error norm of the stabilized response compared to the analytic solution is 2.5%.
 [http://dx.doi.org/10.1121/1.4774377]

PACS number(s): 43.20.Px, 43.20.Rz [NAG] Pages: 1237–1244

I. INTRODUCTION

The time domain boundary element method (TBEM), which calculates the Kirchhoff integral based on the time marching scheme, can directly solve various transient wave propagation problems.[1,2] However, this method suffers from the well-known exponentially diverging instability due to unstable high order eigenmodes, of which poles lie outside a unit circle due to numerical approximation errors.[3,4] Also, calculation for the exterior problem is to be always associated with the non-uniqueness problem, either frequency domain boundary element method (BEM) or TBEM. It is because the Kirchhoff integral includes fictitious internal modes of the radiator in the same manner as the frequency domain calculation based on the Helmholtz integral.

To overcome both the non-uniqueness problem and exponentially diverging instability in TBEM, the time domain Burton-Miller approach has been proposed.[5,6] This method employs a linear combination of the Kirchhoff integral and its normal derivative in the same way as the original frequency domain method.[7] This linear combination suppresses the fictitious internal modes at all frequencies robustly and theoretically. However, the time domain Burton-Miller method still adopts the recursive formulation in which poles can be located outside a unit circle due to uncertain numerical errors. From this reason, the numerical stability cannot be generally assured. Besides, large calculation efforts are needed for executing the hyper singular integral.

The simplest technique in the frequency domain calculation is the CHIEF (Combined Helmholtz Integral Equation Formulation) method, which includes zero pressure constraint equations for additional interior points.[8] Although this method is effective only on low and intermediate frequencies, i.e., in the modal domain, the remaining fictitious internal modes in a high frequency range are not crucial to the fidelity of the solution. It is because the fidelity of a high frequency solution has already been degraded due to the finiteness of element size that increases numerical approximation errors with frequency. However, in the time domain calculation, the response often suffers the exponentially diverging instability caused by some unstable high order fictitious modes even if low order fictitious modes are fully suppressed. Due to this reason, the CHIEF method has been hardly realized in time domain. As a rare trial, the CHIEF constraint equations at all time steps are solved in the non-iterative one-step calculation.[9] However, it does not seem to be a proper method if it is to be used for the time stepping calculation, and a much larger calculation effort is required to deal with a huge overdetermined matrix. Because the algorithm structure of this previous work is simple, further development of the computational method may yield a promising result.

In this paper, a time domain CHIEF method is suggested to stabilize the TBEM calculation for exterior problems. This method includes additional zero pressure constraint equations for the interior points inside the closed body considering the shortest retarded time between the boundary nodes and an interior point. To stabilize the remaining unstable high order fictitious internal modes the filtering method based on the eigen-analysis[10] is used, in which troublesome components are selectively adjusted after projecting the TBEM response onto the eigenspace. In contrast to the previously suggested solution using the Burton-Miller approach, the present method does not involve the hyper singularity and always satisfies the necessary condition to stabilize the unstable poles causing the exponential divergence. The

[a)]Author to whom all correspondence should be addressed. Electronic mail: J.G.Ih@kaist.ac.kr

suggested method is verified with the stabilized results from the calculation of the transient sound field from an impulsively pulsating sphere.

II. TIME DOMAIN CHIEF APPROACH

The time domain acoustic BEM is based on the Kirchhoff integral equation as[1]

$$c(\boldsymbol{r}_0)p(\boldsymbol{r}_0,t_0)=\frac{1}{4\pi}\int_S\left[\frac{1}{R_s^2}\frac{(\boldsymbol{r}_0-\boldsymbol{r}_s)\cdot\boldsymbol{n}}{R_s}\left\{p(\boldsymbol{r}_s,t_{\text{ret}})+\frac{R_s}{c_0}\frac{\partial p}{\partial t}(\boldsymbol{r}_s,t_{\text{ret}})\right\}-\frac{1}{R_s}\frac{\partial p}{\partial n}(\boldsymbol{r}_s,t_{\text{ret}})\right]dS-\frac{\gamma(\boldsymbol{s},t_0-\|\boldsymbol{r}_0-\boldsymbol{s}\|/c_0)}{4\pi\|\boldsymbol{r}_0-\boldsymbol{s}\|},\tag{1}$$

where $c(\boldsymbol{r}_0)$ is the solid angle at field point $\boldsymbol{r}_0$, t_0 is the current time for calculation, $p(\boldsymbol{r},t)$ is the pressure at location $\boldsymbol{r}$ and at time t, S is the domain boundary, R_s is the distance between the field point $\boldsymbol{r}_0$ and the surface point $\boldsymbol{r}_s$ ($R_s=|\boldsymbol{r}_0-\boldsymbol{r}_s|$), t_{ret} is its corresponding retarded time ($t_{\text{ret}}=t_0-R_s/c_0$), c_0 is the speed of sound, $\boldsymbol{n}$ is the unit normal vector toward the acoustic domain of concern, $(\partial/\partial n)$ is the normal derivative on the surface, and γ is an external source function of the point source located at $\boldsymbol{s}$.

By using the conventional BEM technique and taking all boundary nodes as field points, the surface Kirchhoff integral equation can be approximated in a discrete form as follows:[2]

$$\boldsymbol{C}\boldsymbol{P}_n=\sum_{i=0}^{W+2}\left[\boldsymbol{\alpha}_i\boldsymbol{P}_{n-i}+\boldsymbol{\beta}_i\left(\frac{\partial\boldsymbol{P}_{n-i}}{\partial t}\right)+\boldsymbol{\gamma}_i\left(\frac{\partial\boldsymbol{U}_{n-i}}{\partial t}\right)\right]+\boldsymbol{P}_n^i.\tag{2}$$

Here, $\boldsymbol{C}$ is the diagonal matrix containing the solid angles at boundary nodes, $\boldsymbol{P}_n$ and $\boldsymbol{U}_n$ are the surface pressure and velocity vectors at the discrete time $n\Delta t$, respectively, Δt is a time step size, $\boldsymbol{\alpha}_i$, $\boldsymbol{\beta}_i$, and $\boldsymbol{\gamma}_i$ denote the coefficient matrices for the surface variables at $(n-i)\Delta t$, W is the maximum retarded time steps related to the longest distance between boundary nodes, and $\boldsymbol{P}_n^i$ is an incident surface pressure vector from the external point source at $n\Delta t$.

Similar to the frequency domain BEM case, the time domain CHIEF approach uses additional zero-pressure constraint equations for some selected interior points inside the radiator surface. However, the time domain approach does not constrain the steady state surface variables but it constrains the responses at the present time $n\Delta t$ by considering the shortest retarded time, $l_C\Delta t$, between all boundary nodes and the interior CHIEF point $\boldsymbol{r}_C$. In other words, the pressure at the additional interior CHIEF point at $(n+l_C)\Delta t$ is set to be zero as follows:

$$p(\boldsymbol{r}_C,(n+l_C)\Delta t)=\frac{1}{4\pi}\int_S\left[\frac{1}{R_s^2}\frac{(\boldsymbol{r}_C-\boldsymbol{r}_s)\cdot\boldsymbol{n}}{R_s}\left\{p(\boldsymbol{r}_s,t_{\text{ret}})+\frac{R_s}{c_0}\frac{\partial p}{\partial t}(\boldsymbol{r}_s,t_{\text{ret}})\right\}+\frac{\rho}{R_s}\frac{\partial u}{\partial t}(\boldsymbol{r}_s,t_{\text{ret}})\right]dS=0.\tag{3}$$

Equation (3) can be discretized as

$$\boldsymbol{0}=\sum_{i=0}^{W+2}\left[\boldsymbol{\alpha}_i^C\boldsymbol{P}_{n-i}+\boldsymbol{\beta}_i^C\left(\frac{\partial\boldsymbol{P}_{n-i}}{\partial t}\right)+\boldsymbol{\gamma}_i^C\left(\frac{\partial\boldsymbol{U}_{n-i}}{\partial t}\right)\right],\tag{4}$$

where $\boldsymbol{\alpha}_i^{\text{C}}$, $\boldsymbol{\beta}_i^{\text{C}}$, and $\boldsymbol{\gamma}_i^{\text{C}}$ denote the coefficient matrices for the CHIEF equation. One can see that only the unknown surface pressure vector $\boldsymbol{P}_n$ at the current time step can be constrained by using a time delay $l_C\Delta t$. A longer or shorter time delay than $l_C\Delta t$ cannot be used in the time stepping TBEM algorithm because their constrained equations include the responses at the incoming time steps or already calculated known responses at previous time steps. Combining Eqs. (2) and (4), the overall equation can be formulated in an overdetermined form as

$$\begin{bmatrix}\boldsymbol{C}\\ \boldsymbol{0}\end{bmatrix}\boldsymbol{P}_n=\sum_{i=0}^{W+2}\left\{\begin{bmatrix}\boldsymbol{\alpha}_i\\ \boldsymbol{\alpha}_i^C\end{bmatrix}\boldsymbol{P}_{n-i}+\begin{bmatrix}\boldsymbol{\beta}_i\\ \boldsymbol{\beta}_i^C\end{bmatrix}\left(\frac{\partial\boldsymbol{P}}{\partial t}\right)_{n-i}+\begin{bmatrix}\boldsymbol{\gamma}_i\\ \boldsymbol{\gamma}_i^C\end{bmatrix}\left(\frac{\partial\boldsymbol{U}}{\partial t}\right)_{n-i}\right\}+\begin{bmatrix}\boldsymbol{P}_n^i\\ \boldsymbol{0}\end{bmatrix}.\tag{5}$$

Restructuring Eq. (5), one can obtain the following equation:

$$\sum_{i=0}^{m}\boldsymbol{\psi}_i\boldsymbol{P}_{n-i}=\sum_{i=0}^{m}\boldsymbol{\phi}_i\boldsymbol{U}_{n-i}+\begin{bmatrix}\boldsymbol{P}_n^i\\ \boldsymbol{0}\end{bmatrix}.\tag{6}$$

Here, $m\Delta t$ is the maximum retarded time, which is related to the geometric time delay of the longest distance between boundary nodes and the numerical time delay due to both temporal discretization and interpolation, and $\boldsymbol{\psi}_i$ and $\boldsymbol{\varphi}_i$ are rearranged non-square coefficient matrices. Equation (6) can be expressed as

$$\boldsymbol{P}_n=\boldsymbol{\psi}_0^{-1}\left[-\sum_{i=1}^{m}\boldsymbol{\psi}_i\boldsymbol{P}_{n-i}+\sum_{i=0}^{m}\boldsymbol{\phi}_i\boldsymbol{U}_{n-i}+\begin{bmatrix}\boldsymbol{P}_n^i\\ \boldsymbol{0}\end{bmatrix}\right].\tag{7}$$

It shows that the unknown radiated or scattered sound field $\boldsymbol{P}_n$ at the current time step can be calculated from the incident surface pressure and velocity vector at the current time step and the vectors of previous surface variables within the maximum time step. Mathematically, this final formulation adopts the recursive, discrete convolution sum of a multi-input multi-output (MIMO) infinite impulse response (IIR) system in the same manner as the original TBEM formulation.[10] Although this MIMO IIR system enables an efficient, direct calculation of time response, the recursive structure itself often causes the instability that diverges exponentially. The eigensolutions of this MIMO IIR system represent natural internal modes for interior problems and the fictitious internal modes for exterior problems. When the numerical approximation error exists, the poles of some of the eigensolutions can be outside a unit circle in complex domain.

If the suggested CHIEF method is used, the low order fictitious modes within the reliable frequency range, which are determined by the characteristic size of the boundary element, can be damped in full extent. In comparison with the time domain Burton-Miller method,[5] the present CHIEF

method has a merit that the hyper singular integral needs not to be evaluated. However, the TBEM calculation after using the suggested CHIEF method may suffer the exponentially diverging instability yet, due to remaining unstable high order fictitious modes. High order fictitious modes are prone to be amplified due to the additional numerical error by expanding the system in an over-determined manner. Such remaining instability at high order modes can be stabilized by the filtering method in Sec. III.[10]

III. FILTERING METHOD BASED ON EIGEN-ANALYSIS

A. Eigen-analysis

The recursive MIMO IIR formulation of Eq. (7) can be rewritten as[11]

$$\begin{bmatrix} \boldsymbol{P}_n \\ \boldsymbol{P}_{n-1} \\ \vdots \\ \vdots \\ \boldsymbol{P}_{n-m} \end{bmatrix} = - \begin{bmatrix} \boldsymbol{\psi}_0^+\boldsymbol{\psi}_1 & \boldsymbol{\psi}_0^+\boldsymbol{\psi}_2 & \cdots & & \boldsymbol{\psi}_0^+\boldsymbol{\psi}_m \\ \boldsymbol{I} & \boldsymbol{0} & & \cdots & \boldsymbol{0} \\ \boldsymbol{0} & \boldsymbol{I} & \boldsymbol{0} & \cdots & \vdots \\ \vdots & \boldsymbol{0} & \cdots & \boldsymbol{0} & \vdots \\ \boldsymbol{0} & \cdots & \boldsymbol{0} & \boldsymbol{I} & \boldsymbol{0} \end{bmatrix} \times \begin{bmatrix} \boldsymbol{P}_{n-1} \\ \boldsymbol{P}_{n-2} \\ \vdots \\ \vdots \\ \boldsymbol{P}_{n-(m+1)} \end{bmatrix} + \begin{bmatrix} \boldsymbol{I} \\ 0 \\ \vdots \\ \vdots \\ 0 \end{bmatrix} \cdot \boldsymbol{\psi}_0^+ \left[\sum_{i=0}^{m} \boldsymbol{\phi}_i \boldsymbol{U}_{n-i} + \begin{bmatrix} \boldsymbol{P}_n^i \\ \boldsymbol{0} \end{bmatrix} \right]. \tag{8}$$

The above equation can be simply expressed as

$$\langle \boldsymbol{P} \rangle_n = \boldsymbol{M} \langle \boldsymbol{P} \rangle_{n-1} + \langle \boldsymbol{U} \rangle_n, \tag{9}$$

where $\langle \boldsymbol{U} \rangle_n$ is given by boundary conditions and the external source function, $\langle \boldsymbol{P} \rangle_n$ represents the sequence of surface pressure vectors during the maximum time delay, and $()^+$ represents a Moore-Penrose pseudoinverse. The eigensolutions of the single iterative matrix $\boldsymbol{M}$ determine the characteristics of the fictitious internal modes in TBEM calculation. The eigenvector describes the time marching radiation mode shape of the fictitious internal mode. Also, the eigenvalue λ_i, which represents the change rate of the corresponding mode per single time step, determines the modal frequency and decay rate.[4,10] Exponentially diverging instability occurs when the magnitude change rate $|\lambda|$ becomes larger than 1 due to numerical approximation errors.[11]

B. Filtering for stabilization

To stabilize the exponentially diverging instability caused by the remaining unstable high order fictitious modes, the filtering method based on the eigen-analysis[10] is used. The time response can be expanded into the eigenspace and its complementary space as follows:

$$\langle \boldsymbol{P} \rangle_n = \left[\sum_{i=1}^{N} d_i(n\Delta t) \cdot \langle \boldsymbol{u} \rangle_i \right] + (\boldsymbol{I} - \langle \boldsymbol{U} \rangle \langle \boldsymbol{U} \rangle^+) \langle \boldsymbol{P} \rangle_n. \tag{10}$$

Here, $d_i(n\Delta t)$ is the ith modal coefficient at $n\Delta t$, $\langle \boldsymbol{u} \rangle_i$ is the ith eigenvector, N is the number of total eigenmodes, $\langle \boldsymbol{U} \rangle$ is the eigenspace, i.e., the set of all eigenvectors, and $(I\text{-}\langle \boldsymbol{U} \rangle \langle \boldsymbol{U} \rangle^+)$ is its complementary space. In this case, the modal components can be filtered as

$$\langle \tilde{P} \rangle_n = \left[\sum_{i=1}^{N} d_i(n\Delta t) \cdot F_i \cdot \langle \boldsymbol{u} \rangle_i \right] + (\boldsymbol{I} - \langle \boldsymbol{U} \rangle \langle \boldsymbol{U} \rangle^+) \langle \boldsymbol{P} \rangle_n, \tag{11}$$

where $\{\tilde{P}\}_n$ denotes the filtered response and F_i is the filter coefficient representing an artificial damping to the ith eigenmode. Then, the sequential time response at the next time step can be given by

$$\langle \boldsymbol{P} \rangle_{n+1} = \boldsymbol{M} \langle \tilde{\boldsymbol{P}} \rangle_n = \left[\sum_{i=1}^{N} d_i(F_i \lambda_i) \langle \boldsymbol{u} \rangle_i \right] + \boldsymbol{M}(\boldsymbol{I} - \langle \boldsymbol{U} \rangle \langle \boldsymbol{U} \rangle^+) \langle \boldsymbol{P} \rangle_n. \tag{12}$$

One can find that the magnitude change rate is replaced by $F \cdot |\lambda|$. Thus, by setting $F \cdot |\lambda|$ to be less than 1, the necessary stability condition for the magnitude of the eigenvalue can be generally satisfied. Equation (12) can be rewritten in a matrix form as

$$\langle \boldsymbol{P} \rangle_{n+1} = \boldsymbol{M}' \langle \boldsymbol{P} \rangle_n = \boldsymbol{M}[\langle \boldsymbol{U} \rangle \boldsymbol{F} \langle \boldsymbol{U} \rangle^+ + (\boldsymbol{I} - \langle \boldsymbol{U} \rangle \langle \boldsymbol{U} \rangle^+)] \langle \boldsymbol{P} \rangle_n. \tag{13}$$

Here, $\boldsymbol{F}$ is the diagonal filter matrix, of which diagonal entries are F_i. It shows that the calculation at the next time step can be progressed by only the modified single iterative matrix. In other words, the procedure of modal decomposition, filtering, and expansion is not needed to be executed at each time step.

If the troublesome eigenvalues are replaced by those less than one, the exponentially diverging instability can be avoided. In the viewpoint of fidelity, improvement can be attained by modifying troublesome eigenvalues to be closer to a unit circle. However, the amount of improvement is not very influential because the finiteness of the element and time step has already caused the degradation of fidelity of solutions at such high frequencies. On the other hand, the low order unstable modes could not be stabilized even after using the spectral filtering because the proper determination of their filter coefficient is nearly impossible without degrading the fidelity of the solution. More fine mesh and smaller time step are needed to reduce the numerical discretization errors further. With the same rationale, for the exterior problems the filtering method could not be used exclusively without the proposed time domain CHIEF technique for suppressing the low order fictitious modes. In this work, after

using a sufficiently fine mesh and time step as well as applying the proposed CHIEF method, the eigenvalues of the remaining unstable high order fictitious modes are selectively adjusted to become 1 ($F\cdot|\lambda|=1$), and the other stable modes are not changed at all ($F=1$).

IV. TEST EXAMPLE AND DISCUSSIONS

Sound radiation from an impulsively pulsating sphere is dealt with as a test example. The radius of a sphere is 0.25 m, and the boundary element model is composed of 458 nodes and 228 quadratic triangular elements. The maximum element size is 0.150 m, so the high frequency limit for a reliable frequency range is 0.77 kHz under the $\lambda/3$ criterion with a maximum modeling error of 5%.[12] The time step size Δt is 0.0625 ms ($f_s=16$ kHz), of which the ratio to the minimum distance between nodes, i.e., $c_0\Delta t/\Delta h_{\min}$, is 1.03. An octave band impulse, which is the inverse Fourier transform of an octave bandpass filter centered at 0.5 kHz, is given as the input normal velocities on all boundary nodes. The analytically calculated modal parameters of the lowest ten fictitious modes are summarized in Table I. In Table I, the index (l,n,m) denotes the mode shape of a fictitious internal mode expressed in spherical coordinate (r,θ,ψ): $\Phi_{lmn}=[c_1\cdot\cos(m\psi)+c_2\cdot\sin(m\psi)]\cdot P_n^m(\cos(\theta))\cdot j_n(kr)$. Here, c_1, c_2 are arbitrary constants, P_n^m denotes the associated Legendre polynomials, a is the radius of spherical radiator, and ka is the lth zero of the spherical Bessel function j_n.

As an initial attempt to find any clue for the proper location and number of CHIEF points, the sound radiation from a harmonically pulsating sphere with a frequency of the (1,0,0) fictitious mode is calculated. Figure 1 shows the magnitude of the radiated sound varying the radial distance of a single CHIEF point, and a comparison is made with the analytic solution. In this calculation, the spectral filtering is used to solve the exponentially diverging instability caused by the remaining high order unstable modes. Like the frequency domain BEM, the suggested time domain CHIEF technique suppresses the target fictitious mode to be smaller and smaller as the additional interior point becomes near the anti-nodal point, i.e., the center of the sphere. The error becomes less than 5% for $r\le 0.025$ m. However, one can see that the effect of the fictitious mode is minimum at $r=0.02$ m, which is not an anti-nodal point. It is perhaps due to the fact that the numerical dissipation stemmed from discretization still persists even after the fictitious modes are fully eliminated by the CHIEF method. Figure 2 shows the change of frequency and decay rate of the first fictitious mode after employing the CHIEF method with the variation of the position of a single CHIEF point. As the CHIEF point approaches the anti-nodal point, the fictitious mode of concern becomes more dissipative and its modal frequency becomes lower, which is already well known in the frequency domain CHIEF method. On the other hand, as shown in Fig. 3, the exponentially diverging instability becomes steeper and the frequency range of unstable modes becomes lower as the radial position of a CHIEF point comes near the center of the sphere. Because their frequencies are nevertheless higher than the high frequency limit of the boundary element model, the spectral filtering is yet allowable.

TABLE I. Characteristics of the lowest ten fictitious internal modes.

(l, n, m)	ka	Freq. (Hz)	Anti-node
(1,0,0)	3.142	687.0	$\|r\|=0$ m
(2,0,0)	6.283	1374.0	$\|r\|=0$, 0.179 m
(1,1,−1), (1,1,0), (1,1,1)	4.493	982.5	$\|r\|=0.116$ m
(1,2,−2), (1,2,−1), (1,2,−1),(1,2,−1), (1,2,2)	5.763	1260.2	$\|r\|=0.145$ m

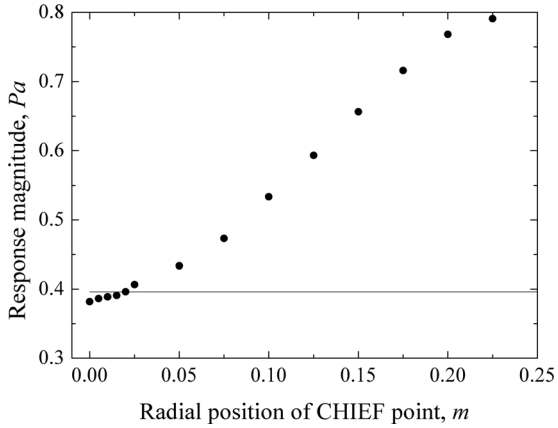

FIG. 1. Magnitude of TBEM response from a harmonically pulsating sphere at a frequency of the first fictitious mode as a function of the radial distance of a single CHIEF point from the center of sphere: •, TBEM; —, analytic solution.

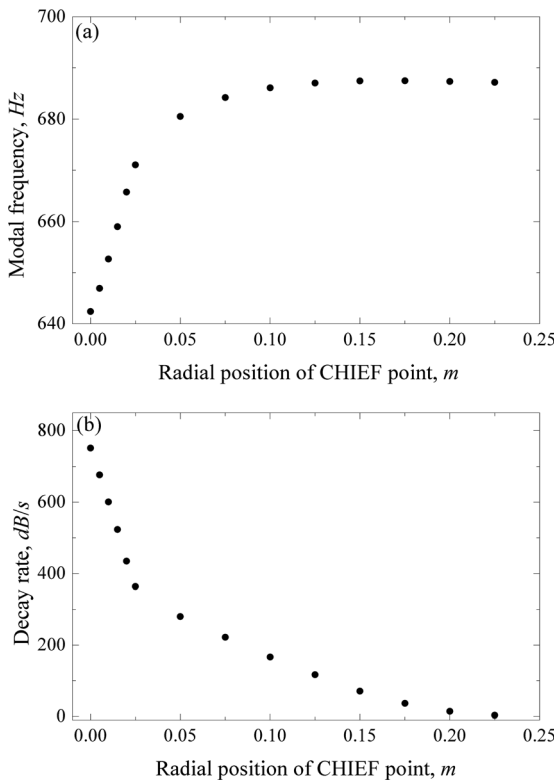

FIG. 2. Modal parameters of the first pulsating fictitious mode as a function of the radial distance of a single CHIEF point from the center of sphere. (a) Modal frequency and (b) decay rate.

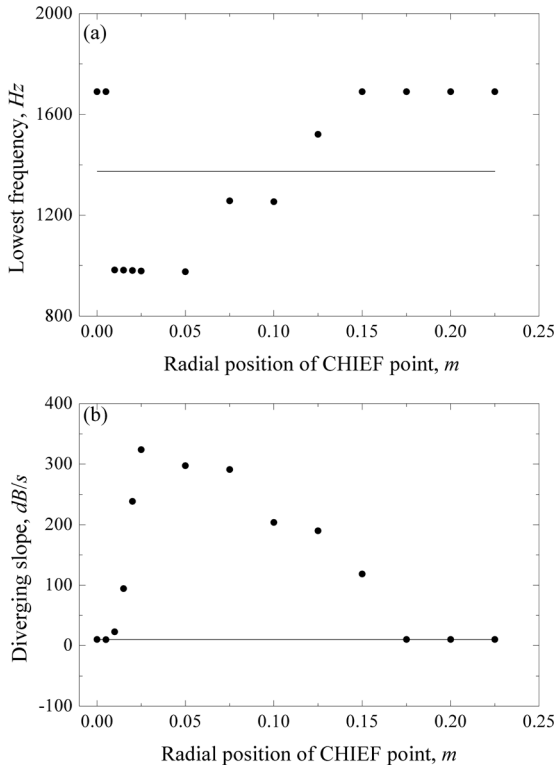

FIG. 3. Characteristics of unstable modes as a function of the radial distance of a single CHIEF point from the center of sphere: •, TBEM with the CHIEF method; —, TBEM without the CHIEF method. (a) The lowest frequency and (b) diverging slope.

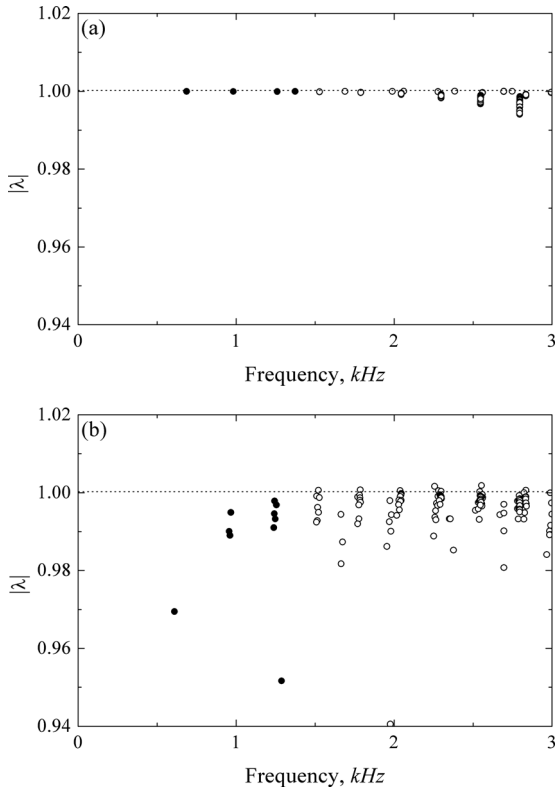

FIG. 4. Magnitudes of eigenvalues and frequencies of the eigenmodes of TBEM calculation: •, the lowest ten modes in Table I; [○], the other high order modes. (a) Without the CHIEF method and (b) with the CHIEF method.

In Table II one can find that a single good CHIEF point at $r = 0.02$ m is sufficient to suppress the first fictitious mode. In this test, bad CHIEF points are located near the nodal surface. With an increased number of bad CHIEF points, the decay rate of the target fictitious mode increases in a similar way to that of TBEM calculation with a single good CHIEF point. However, the error is still higher than 10%, and the fictitious modal frequency is little changed. Table II exhibits the computation results by exclusive use of the spectral filtering focused on the lowest fictitious mode. Although the decay rate is set to be identical to that for the calculation with only *good* CHIEF points, most responses are too much damped down. This is because there is no physical based strategy on how to change the eigenvalues related to such low order fictitious modes.

Anyway, this test result suggests that the number of CHIEF points is an important factor for effectively suppressing the fictitious modes although a large number of CHIEF points would invoke an uneconomical computation. For more complicated models in the majority of cases, there is no choice but to use randomly distributed CHIEF points because anti-nodal locations are usually unknown. Thus, in this simulation, 30 randomly distributed CHIEF points are tested based on the assumption that their optimal locations are unknown. Figure 4 shows modal parameters of dominant fictitious internal modes before and after applying the time domain CHIEF approach with 30 randomly distributed additional points. One can observe that the fictitious modes calculated by the original TBEM before employing the present

TABLE II. Performance according to the CHIEF point selection method and the exclusive use of spectral filtering.

		First pulsating mode		Unstable modes		Harmonic response at 687 Hz	
		f_i (Hz)	D_i (dB/s)	min(f_i)	Diverging slope (dB/s)	Analytic	TBEM
Number and condition of CHIEF points	0 bad, 0 good	687.0	841.3	1374.1	10.0	0.3960	0.8059
	0 bad, 1 good	665.7	434.6	979.8	238.8		0.3962
	1 bad, 0 good	687.4	14.2	1689.5	10.0		0.7681
	3 bad, 0 good	684.6	349.7	1255.9	299.5		0.4570
	5 bad, 0 good	686.2	451.9	1528.0	261.6		0.4532
	5 bad, 1 good	665.8	841.3	1527.9	264.7		0.3991
Use of spectral filtering only		687.0	434.6	1374.1	10.0		0.1964
		687.0	841.3	1374.1	10.0		0.0941

CHIEF method appear at the analytically calculated modal frequencies of the fictitious internal modes satisfying the zero of the spherical Bessel function, $j_n(ka)=0$. It is also noted that the low order fictitious modes are hardly dissipated as the magnitudes of their eigenvalues are nearly 1. However, the dissipation is increased gradually with frequency due to the increasing numerical approximation errors. The TBEM calculation without using the CHIEF method involves 32 unstable modes for a frequency range of 1.4 to 2.8 kHz, which is far beyond the reliable calculation range of the boundary element model. Moreover, because the magnitudes of their eigenvalues are very close to 1, in which $|\lambda|_{\max}$ is $1+7.3\times10^{-5}$ and its corresponding decay rate,[10] D, is -10.1 dB/s, the onset of exponentially diverging instability is delayed to a very late time.

After employing the suggested CHIEF method, the low order fictitious modes are fully damped down, as the magnitudes of eigenvalues of the lowest 10 fictitious internal modes range from 0.9517 to 0.9979, which corresponds to the decay rate range of 295 to 6890 dB/s. It is also noted that the frequencies of fictitious internal modes become lower than those of the original TBEM calculation without using CHIEF method. The number of unstable modes is 20 and the slope of exponentially diverging instability becomes much steeper than that of the original TBEM calculation without using the CHIEF method: $|\lambda|_{\max}=1.0019$, $D=-259$ dB/s. However, because their frequencies are in the range of 1.5 to 2.8 kHz, which is far higher than the high frequency limit of the boundary element model, further stabilization can be done by using the filtering method in Sec. III.[9]

Figure 5 represents the calculated time response for a transiently pulsating sphere with an octave band impulse excitation centered at 0.5 kHz and its frequency spectrum before employing the suggested CHIEF method, which are compared with the analytical solution, i.e., the inverse Fourier transform of the analytical spectrum. Although the calculated response in early time steps agrees well with the analytical solution, the effect of fictitious internal resonance can be seen clearly in the late time steps as a ringing. Such a fictitious resonant component is also contained in the frequency spectrum. The resonant frequencies are actually that of the first pulsating fictitious mode, i.e., the (1,0,0) mode in Table I. Because of very slowly diverging slopes of unstable modes as previously mentioned in Fig. 4, the onset of exponentially diverging instability is not observed. As a parameter of precision, the relative error norm is given by

$$e=\left[\sqrt{\sum_i (p_A[i\Delta t]-p_T[i\Delta t])^2}\Big/\sqrt{\sum_i (p_A[i\Delta t])^2}\right]\times 100(\%), \tag{14}$$

where p_A and p_T denote the analytic solution and the TBEM result, respectively. In the results before applying the suggested CHIEF method, the average of relative error norm of the surface pressure at all boundary nodes is 31.4% due to the presence of fictitious resonance in the late time steps.

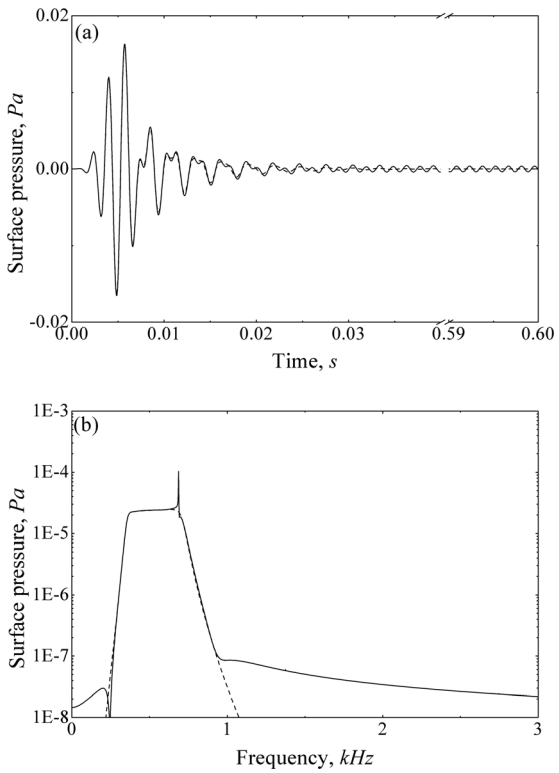

FIG. 5. Comparison of the analytic solution with the calculated surface pressure from the original formulation before using the time domain CHIEF method: ——, TBEM; - - - - - -, analytic solution. (a) Time response and (b) frequency spectrum.

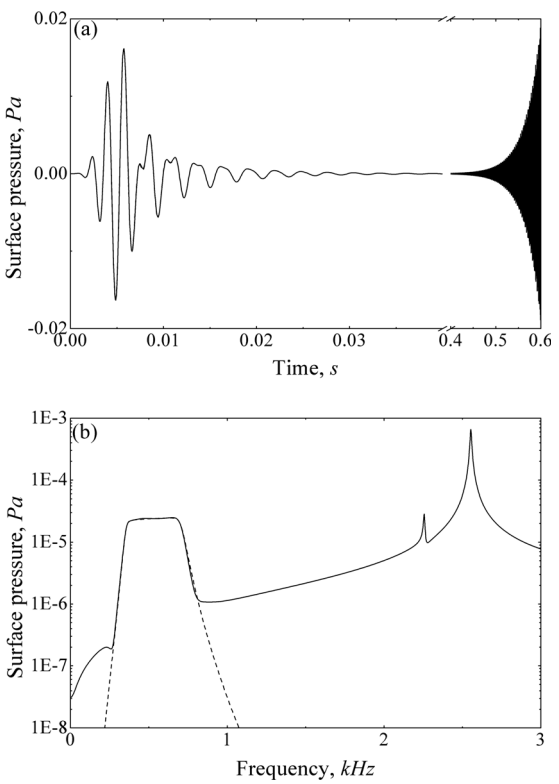

FIG. 6. Comparison of the analytic solution with the calculated response of TBEM by using the time-domain CHIEF technique: ——, TBEM; - - - - - -, analytic solution. (a) Time response and (b) frequency spectrum.

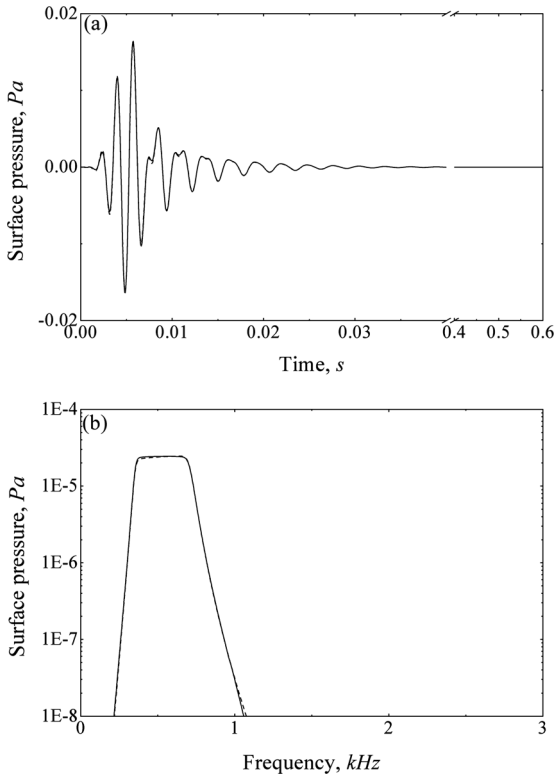

FIG. 7. Comparison of the analytic solution with the stabilized response of TBEM by nullifying the remaining unstable modes (Ref. 10) after using the time domain CHIEF technique: ——, TBEM; - - - - - -, analytic solution. (a) Time response and (b) frequency spectrum.

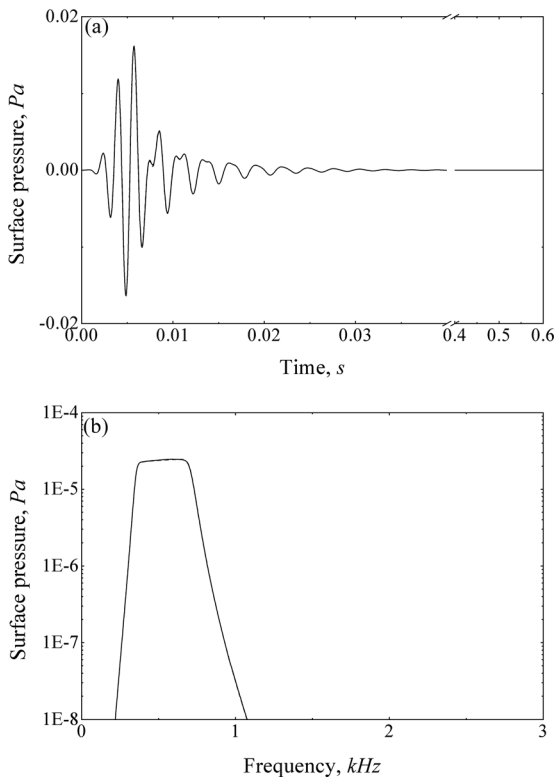

FIG. 8. Comparison of the analytic solution with the stabilized response of TBEM by adjusting the eigenvalues of the remaining unstable modes to be 1 after using the time domain CHIEF technique: ——, TBEM; - - - - - -, analytic solution. (a) Time response and (b) frequency spectrum.

In Fig. 6(a), the calculated response after employing the suggested CHIEF method is depicted in which the resonant components of low order fictitious modes disappear. However, it is observed that the enlarged maximum magnitude of the eigenvalue causes the divergence at late times growing up very rapidly after 0.4 s. Figure 6(b) also shows that their frequencies are beyond the reliable frequency range of the selected boundary element model. For a complete stabilization, such high order unstable modes should be adjusted by using the filtering method[10] which hardly degrades the fidelity of the solution because of their high frequencies. Figure 7 shows the stabilized time response by nullifying the remaining high order unstable modes and its frequency spectrum. The final response agrees very well with the analytic solution and the exponentially diverging instability disappears even at late time steps. The average of relative error norms of the surface pressures at all boundary nodes becomes 3.4%. Figure 8 shows the stabilized results by adjusting the eigenvalues of unstable high order modes to be 1, i.e., $F\cdot|\lambda| = 1$. In this case, the exponentially diverging instability problem is also solved as mentioned in Sec. III. In comparison with the results obtained by nullifying unstable high order modes, the average of relative error norms is reduced to 2.5% because the residue of spectral filtering decreases as the modified eigenvalues become closer to a unit circle in the complex plane.[10] However, the errors in both cases are within the margin of meshing error of $\lambda/3$ criterion, 5%.

V. CONCLUSIONS

In this paper, a method to stabilize the TBEM calculation for exterior problems is suggested. To solve the non-uniqueness difficulty related to the low order fictitious mode, the time domain CHIEF method is suggested by considering the shortest retarded time between boundary nodes and an interior CHIEF point. In addition to the suggested CHIEF method, the filtering method based on the eigen-analysis[10] is recommended to employ to stabilize the exponentially diverging instability caused by the remaining unstable high order fictitious modes at high frequencies.

In the test example, the low order fictitious internal modes within the reliable frequency range are suppressed completely by using the suggested CHIEF method. However, by introducing the CHIEF points, it is found that the slope of exponentially diverging instability becomes much steeper. Those are actually high order fictitious modes at frequencies higher than the high frequency limit of the boundary element model that become the source of the exponential divergence at late times. By adjusting troublesome modes beyond the reliable frequency range, a complete stabilization could be achieved. The average of the relative error norm of the stabilized final response is found to be 2.5%. In comparison with the previously suggested Burton-Miller approach,[5] the present two-step stabilization method does not involve the hyper singularity, and the necessary stability condition for the magnitudes of eigenvalues can always be satisfied.

ACKNOWLEDGMENTS

This work was partially supported by BK21 Project and the NRF Grant (No. 2012R1A2A2A01009874).

[1]P. H. L. Groenenboom, "Wave propagation phenomena," in *Progress in Boundary Element Methods*, edited by C. A. Brebbia (Pentech, London, 1983), Vol. 2, pp. 24–52.
[2]J. L. Dohner, R. Shoureshi, and R. J. Bernhard, "Transient analysis of three dimensional wave propagation using the boundary element method," Int. J. Numer. Methods Eng. **24**, 621–634 (1987).
[3]P. D. Smith, "Instabilities in time marching methods for scattering: Cause and rectification," Electromagnetics **10**, 439–451 (1990).
[4]H. Wang, D. J. Henwood, P. J. Harris, and R. Chakrabarti, "Concerning the cause of instability in time stepping boundary element methods applied to the exterior acoustic problem," J. Sound Vib. **305**, 289–297 (2007).
[5]A. A. Ergin, B. Shanker, and E. Michielssen, "Analysis of transient wave scattering from rigid bodies using a Burton-Miller approach," J. Acoust. Soc. Am. **106**, 2396–2404 (1999).
[6]D. J. Chappell, P. J. Harris, D. Henwood, and R. Chakrabarti, "A stable boundary element method for modeling transient acoustic radiation," J. Acoust. Soc. Am. **120**, 76–80 (2006).
[7]A. J. Burton and G. F. Miller, "The application of integral equation methods to the numerical solution of some exterior boundary-value problems," Proc. R. Soc. London, Ser. A **323**, 201–210 (1971).
[8]H. A. Schenck, "Improved integral formulation for acoustic radiation problems," J. Acoust. Soc. Am. **44**, 41–58 (1968).
[9]M. Stutz, M. Ochmann, and M. Moser, "Improving stability of the transient boundary element method using the CHIEF-Method," on the CD-ROM: *Ljubljana, September 15–18, 2010, 1st EAA—EuroRegio, Congress on Sound and Vibration* (2010).
[10]H.-W. Jang and J.-G. Ih, "Stabilization of time domain acoustic boundary element method for the interior problem with impedance boundary conditions," J. Acoust. Soc. Am. **131**, 2742–2752 (2012).
[11]S. J. Dodson, S. P. Walker, and M. J. Bluck, "Implicitness and stability of time domain integral equation scattering analyses," Appl. Comput. Electromagn. Soc. J. **13**, 291–301 (1998).
[12]S. Marburg, "Six boundary elements per wavelength: Is that enough?" J. Comput. Acoust. **10**, 25–52 (2002).